7. Chapter 7: Development of Chitosan and DNase coated solid lipid nanoparticles encapsulating Anacardic Acid ($Ana_{C15:3}$)

7.1 Materials

Table 7.1: List of chemicals used in the study

S.No	Materials	Suppliers
1.	Glyceryl monostearate	Himedia Ltd, Mumbai, India
2.	Poloxamer 188	Himedia Ltd, Mumbai, India
3.	Chitosan (140 KD M.W. ≥75% Deacetylated)	Sigma-Aldrich, Bangalore, India
4.	Live/Dead cell viability kit (Syto 9/Propidium iodide)	Thermo Fischer Scientific, India
5.	Potassium dihydrogen orthophosphate	S D Fine chem limited, Mumbai, India
6.	Di-sodium hydrogen orthophosphate anhydrous	S D Fine chem limited, Mumbai, India

7.2 Methods

7.2.1 Preparation of Anacardic Acid loaded solid lipid nanoparticles

Anacardic Acid ($Ana_{C15:3}$) loaded SLNs were prepared by using hot homogenization technique with slight modifications (Jenning, Lippacher et al. 2002). Briefly, GMS was heated above its melting point (70°C), followed by the addition of Ana to finally obtain the drug lipid melt. The continuous aqueous phase was prepared by dissolving the poloxamer 188 in hot distilled water maintained at the same temperature (70°C). Further, the hot aqueous continuous phase was transferred slowly to the drug lipid melt under stirring to yield pre-emulsion. Now, the pre-emulsion was subjected to homogenization at 13000 rpm for 20 min using a high-speed homogenizer (T-25 digital ultraturrax, IKA, Germany) followed by sonication at an amplitude of 30% for 10 min using probe sonicator. The final emulsion was then cooled at room temperature to yield the solidified

SLNs. $Ana_{C15:3}$-free SLNs (Blank SLNs) were also prepared similarly without the addition of $Ana_{C15:3}$ (Pandya, Jani et al. 2018). The SLNs were further lyophilized using mannitol (5% w/v) as a cryoprotectant and stored at 2-8°C.

7.2.2 Chitosan and DNase coated SLNs

Chitosan coated SLNs were prepared to obtain positively charged SLNs. Briefly, the chitosan solution (0.5 mg/mL) was prepared by dissolving the required amount of chitosan in 0.1% acetic acid. The resulting solution was further filtered using a 0.45 µm membrane filter (Millex syringe filter, Merck) to eliminate the impurities. The resultant solution was preheated to 70°C and used as the continuous aqueous phase (Luo, Teng et al. 2015). All other preparation parameters were kept unchanged as discussed above. Further, DNase coated SLNs were formulated by dropwise addition of DNase type I (stock of 10 mg/mL in physiological solution (pH 5.0) with continuous stirring to yield 10 µg/mg of lipid used in the formulation (Islan, Tornello et al. 2016).

7.2.3 Characterization of Ana-loaded SLNs

7.2.3.1 Dynamic light scattering (DLS) studies for particle size, polydispersity index, and zeta potential

DLS measurements were performed to determine the particle size (PS), polydispersity index (PDI), and zeta potential (ZP) of the nanoparticles using Delsa™ Nano HC (Beckman Coulter, Inc.USA). The freeze-dried powder was dispersed and diluted with distilled water to achieve the scattering in the instrument sensitivity range. Samples were analyzed in triplicate, and the experimental results were expressed as mean ± standard deviation (Garcês, Amaral et al. 2018).

7.2.3.2 Entrapment efficiency

Entrapment efficiency was determined by the indirect method. The nanoparticle dispersion was centrifuged at 15,000 rpm in a cooling centrifuge (REMI, India, Model

C-24) at 4°C for 30 minutes. The supernatant was diluted suitably with ethanol, and the amount of Anacardic Acid was determined by UV-Spectrophotometer **(**UV-1700 PharmSpec, Shimadzu**)** at a wavelength (λ) 312 nm (Ayan, Yenilmez et al. 2017). Percentage entrapment efficiency (EE %) was calculated from the equation (1) as follows;

$$\text{EE } \% = \frac{\text{The total amount of drug (mg)} - \text{Free drug(mg)}}{\text{The total amount of drug (mg)}} \times 100 \qquad (1)$$

The total amount of drug represents the drug used to fabricate the SLNs

Free drug represents the drug in the supernatant

7.2.3.3 Transmission electron microscopy (TEM)

The $Ana_{C15:3}$-SLNs and $Ana_{C15:3}$-SLNs-CH-DNase dispersions were diluted 10 times with HPLC grade ultrapure water, and a drop of the formulation dispersion spreaded on a collodion coated Cu grid (400 mesh). Excess liquid was wiped out using filter paper. One drop of phosphotungstic acid was also added for staining the nanoparticles and TEM analysis was performed through Tecnai G2 20 TWIN (FEI Company of USA (S.E.A.) PTE, LTD) (Shakeri, Razavi et al. 2019).

7.2.3.4 FT-IR Spectroscopy

FT-IR spectra of $Ana_{C15:3}$, excipients, and $Ana_{C15:3}$ loaded formulations ($Ana_{C15:3}$-SLNs and $Ana_{C15:3}$-SLNs-CH-DNase) were acquired using FT-IR, Bruker Alpha II FTIR Spectrometer (Bruker Corporation, Germany). The test samples were scanned at a spectral range of 500-4000 cm^{-1} using resolution 2 cm^{-1} and 128 scans for each run. The test samples were first ground with KBr powder and compressed to yield pellets to perform the measurement (Sharma, Gupta et al. 2016).

7.2.3.5 X-Ray Diffraction analysis (XRD)

The X-ray diffraction characteristics of the $Ana_{C15:3}$, excipients, and $Ana_{C15:3}$ loaded formulations ($Ana_{C15:3}$-SLNs and $Ana_{C15:3}$-SLNs-CH-DNase) were evaluated using Rigaku Miniflex 600 Desktop X-Ray Diffraction system (Rigaku Corporation, Japan) equipped with HyPix-400 MF 2D hybrid pixel array detector (HPAD). The applied current and voltage were 40 mA and 40 kV, respectively. The results were recorded in the diffraction angle (2θ) range 5–40° having scan rate 10°/min and step size 0.03° (Mulik, Mönkkönen et al. 2010).

7.2.3.6 In-vitro drug release studies

The dialysis bag diffusion method was employed to evaluate the *in-vitro* drug release pattern from $Ana_{C15:3}$-suspension and $Ana_{C15:3}$ encapsulated formulations ($Ana_{C15:3}$-SLNs and $Ana_{C15:3}$-SLNs-CH-DNase). The dialysis bag (Molecular weight cut off: 14000 Dalton) was suspended in a glass beaker having 100 ml phosphate buffer (PBS, pH 6.8) as release media containing 0.1% SLS (solubility of the drug is very poor, and hence 0.1% SLS is added to the buffer to maintain sink condition as well to increase the solubility of the drug in the buffer) maintained at 37±2°C with continuous stirring at 100 rpm. Aliquots of 1 mL from release media were withdrawn at predetermined time intervals (1, 2, 3, 4, 8, 12, and 24 h) and replaced with fresh media (Pandya, Jani et al. 2018). The samples were further diluted and analyzed using a UV-Vis spectrophotometer.

7.2.3.7 Stability study

A stability study was performed to investigate the physical stability of the developed SLNs upon storage. Lyophilized samples were stored at the refrigerated condition (2-8 °C) and room temperature (25±2°C and relative humidity 65±5%) for 90 days.

Parameters like particle size and encapsulation efficiency were analyzed at different time intervals (0, 30, 60, and 90 days) (Luo, Teng et al. 2015).

7.2.3.8 In-vitro cytotoxicity study

HaCaT (human immortalized keratinocytes) cells were employed for the determination of the *in-vitro* cytotoxic effect of SLNs. Briefly, the HaCaT cells were seeded with 3×10^3 cells per well into the culture plate (96-well) and were treated with various test samples ($Ana_{C15:3}$, $Ana_{C15:3}$-SLNs, $Ana_{C15:3}$+DNase, $Ana_{C15:3}$-SLNs-CH, and $Ana_{C15:3}$-SLN-CH-DNase) considering the Ana concentrations *viz.* 50, 25, 12.5, 6.25, 3.125, 1.562, 0.781, 0.390, 0.195 and 0.097 µg/mL. Viable cells were assessed using MTT {3-(4, 5-dimethylthiazol-2-yl)-2,5-diphenyltetrazolium bromide} colorimetric analysis. After 72 h, the supernatants from the culture were replaced with MTT (10%) and incubated for another 3 h at 37°C. The dark blue formazan formed were solubilized by the addition of isopropanol. Further, absorbance at 550 nm was recorded using a microplate reader (MR 680 Bio-Rad) (Mulik, Mönkkönen et al. 2010).

7.2.4 Antimicrobial study

The antimicrobial activity of $Ana_{C15:3}$ and $Ana_{C15:3}$ encapsulated formulations ($Ana_{C15:3}$-SLNs, $Ana_{C15:3}$-SLNs-CH, and $Ana_{C15:3}$-SLNs-CH-DNase) were assessed by estimating minimum inhibitory concentration (MIC) against *S. aureus*. MICs for $Ana_{C15:3}$ and $Ana_{C15:3}$ encapsulated formulations were determined by the broth dilution method. Bacterial suspensions were cultured at 37°C for 24 h and further diluted to yield 1×10^5 CFU/mL. Further, 20 µL of bacterial suspensions (1×10^5 CFU/mL) were mixed with 180 µL Muller Hinton Broth (MHB) comprising different concentrations of the test sample ($Ana_{C15:3}$ suspension and $Ana_{C15:3}$ encapsulated formulations) ranging from 0.097-50 µg/mL in microtiter 96 well plate (Lee, Fu et al. 2017). The $Ana_{C15:3}$ encapsulated formulations were further diluted with the culture media while $Ana_{C15:3}$ suspension was

obtained as an aqueous suspension, containing 1% v/v DMSO. Microtiter well plates were then incubated at temperature 37°C for 24 h, and further turbidity of the test samples was evaluated using a microplate reader (MR 680 Bio-Rad) at 450 nm. The MICs of test samples were considered as the minimum concentration with no observable growth (≤ 0.05 difference in OD 450) investigated following the incubation for 24 h. All the studies were performed in triplicate (Sharma, Gupta et al. 2016).

7.2.4.1 Effect of SLNs on the formation of biofilm (Evaluation of biofilm inhibition potential)

The ability of the test samples to restrict biofilm development by planktonic bacteria was evaluated in this study by investigating biofilm inhibitory effects against *S. aureus* grown in peg lids, applying different concentrations of $Ana_{C15:3}$ and $Ana_{C15:3}$ encapsulated formulations. Briefly, peg lids were placed inside wells of the microplate (96 well) comprising of *S. aureus* suspension (5×10^5 CFU/mL) in LB medium supplemented with 0.25% glucose. Test samples in different drug concentrations (50, 25, 12.5, 6.25, 3.125, 1.562, 0.781, 0.39, 0.195 and 0.097 µg/mL) were used in specified wells. The microplates were further incubated at 37°C for 48 h. Furthermore, the peg lids were removed and washed thrice with PBS to remove loosely adhered planktonic bacteria. Biofilm forming bacteria were recovered in LB media (200 µL) by centrifugation (Remi centrifuge, India) at 2500 rpm. The recovered biofilms were serially diluted and plated on agar plates. Colony-forming units of bacteria were counted after 24 and 48 h (Gade, Patel et al. 2019).

7.2.4.2 Effect of SLNs on mature biofilm (Evaluation of biofilm eradication potential)

Biofilm eradication activity of the test samples was examined by growing *S. aureus* biofilm on the peg lids. In the study, culture plates (96 well, Polystyrene, transparent, and sterile) were employed. Briefly, 200 µL of LB media containing *S. aureus* (0.5×10^6 CFU/mL) was sheathed with the peg lids and incubated for 48 h at 37°C using a rotary

incubator shaker to get the biofilms adhered on the peg lids. The adherence of the biofilms was confirmed through methylene blue dye test. After 48 h, the biofilm adhered peg lids were washed with PBS thrice to rule out the presence of loosely adhered planktonic bacteria. Further, the biofilm adhered peg lids were transferred to another culture plate having LB media with test samples of various serially diluted concentrations *viz.* 50, 25, 12.5, 6.25, 3.125, 1.562, 0.781, 0.390, 0.195 and 0.097µg/mL. The culture plates were again incubated for 24 h at 37°C, and the biofilms adhered to peg lids were recovered by placing the peg lids on a fresh culture plate containing media and then sonicated (Gade, Patel et al. 2019). Now, the recovered cells were serially diluted, cultured on an agar plate to count the CFUs. Further, the biofilms were treated with subsequent doses for 48 h to evaluate the biofilm eradication efficiency of the drug and formulations (Shakeri, Razavi et al. 2019).

7.2.4.3 Microscopic study of biofilm

S. aureus biofilms were grown on the microscopic glass coverslips (18 mm diameter) immersed inside the wells of 12 well culture plate as mentioned in the previous study. Briefly, coverslips having biofilms adhered on its surface were lifted out of the culture plates following 48 h growth period and carefully washed using PBS to get rid of the loosely adhered cells. Furthermore, the glass coverslips were again placed inside the culture plate with fresh LB media followed by treatment with different test samples. After 48 h of treatment, the glass coverslips were taken out from the wells of the culture plate. The bacterial cells of the biofilms were fixed using 4% w/v paraformaldehyde followed by staining with LIVE/ DEAD BacLight Bacterial Viability Kit (Thermo Fischer, India) in the dark environment as per the guidelines of the manual (6 µM SYTO9 and 30 µM Propidium Iodide). The test samples were further examined under a confocal laser scanning microscope (CLSM) (Zeiss, Germany). Sections of the test samples were

scanned at two wavelengths (488 and 560 nm) using a 40X magnification lens. The z-stack photographs were captured at z step size of 2.63 µ (Gade, Patel et al. 2019). At the end, the acquired images were assessed using Image J software (COMSTAT-2.1) to finally get the thickness and biomass of biofilms over treatment with different test samples. Images in triplicate were acquired from the various regions of each tested group. The data represented in the manuscript an average of three recorded values.

7.2.5 Statistical analysis

All the experiments were performed in triplicate (n=3), and the data expressed as mean± standard deviation (SD). Statistical analyses of data were performed using software Graph Pad Prism 5.01 (Graph Pad Software Inc. San Diego, USA).

7.3 Results and Discussion

7.3.1 Characterization of Ana$_{C15:3}$-SLNs

The SLNs were prepared and were further engineered through DNase and Chitosan coating. All the parameters were evaluated to ensure the efficacy of the developed formulation. The detailed outcomes upon evaluation of the developed SLNs are discussed in this section.

7.3.1.1 Particle Size, Polydispersity Index and zeta potential

The particle size, PDI, and zeta potential of Ana$_{C15:3}$-SLNs, Ana$_{C15:3}$-SLNs-CH, as well as Ana$_{C15:3}$-SLNs-CH-DNase, are listed in (Table 7.2). Small-sized nanoparticles add the advantage of efficient internalization and hence, enhance activity. Ana$_{C15:3}$-SLNs showed negative zeta potential while Ana$_{C15:3}$-SLNs following the coating of chitosan showed positive zeta potential.

Table 7.2: Data representing particle size, PDI, and zeta potential of different formulations.

	Particle size (nm)	PDI	Zeta potential (mV)
$Ana_{C15:3}$-SLNs	203.6±3.05	0.277±0.02	-21.4±2.81
$Ana_{C15:3}$-SLNs-CH	206.5±4.67	0.316±0.04	+16.8±2.16
$Ana_{C15:3}$-SLNs-CH-DNase	212.8±4.21	0.285±0.04	+13.5±1.92

7.3.1.2 Entrapment Efficiency (EE %)

EE% of the $Ana_{C15:3}$-SLNs, $Ana_{C15:3}$-SLNs-CH, and $Ana_{C15:3}$-SLNs-CH-DNase formulations were found to be 76.4±1.9, 74.6±2.1, and 73.8±1.23%, respectively. Higher entrapment of $Ana_{C15:3}$ in SLNs is attributed to the lipophilic nature of $Ana_{C15:3}$ and its higher solubility in the selected lipid.

7.3.1.3 Transmission Electron Microscopy (TEM)

The surface morphology of the SLNs was determined using TEM (Figure 7.1). Formulated SLNs were found to be spherical, having a smooth surface and uniform size. It is clear from the images that particles are well separated from each other, confirming the stability of the developed SLNs.

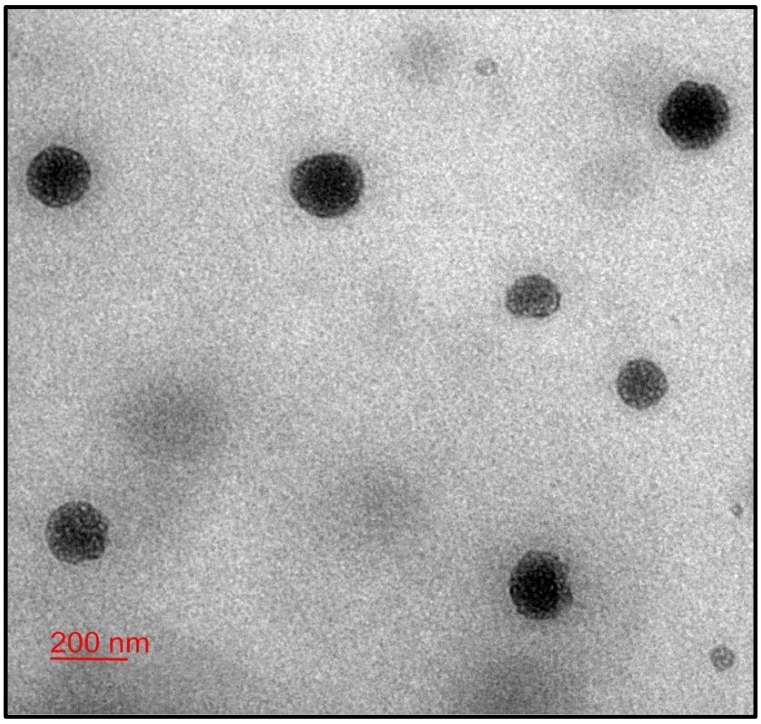

Figure 7.1: TEM image of $Ana_{C15:3}$-SLNs-CH-DNase

7.3.1.4 FT-IR spectroscopy

FT-IR spectra of pure $Ana_{C15:3}$ (Figure 7.2 A) demonstrated intense peaks at 3420 and 1304 cm^{-1} (Ar-OH), 3400-2400, 1645 cm^{-1} and 1304 cm^{-1} (-COOH), 3009 cm^{-1} (Ar-H and vinyl-H), 2924 and 2849 cm^{-1} (aliphatic C-H), 1607 cm^{-1} (aliphatic C=C), and 1446 cm^{-1} (aromatic C=C). Furthermore, all the transmittance peaks corresponding to $Ana_{C15:3}$ were also present in $Ana_{C15:3}$-SLNs and $Ana_{C15:3}$-SLNs-CH-DNase (Figure 7.2 B&D), suggesting compatibility of $Ana_{C15:3}$ with other formulation components.

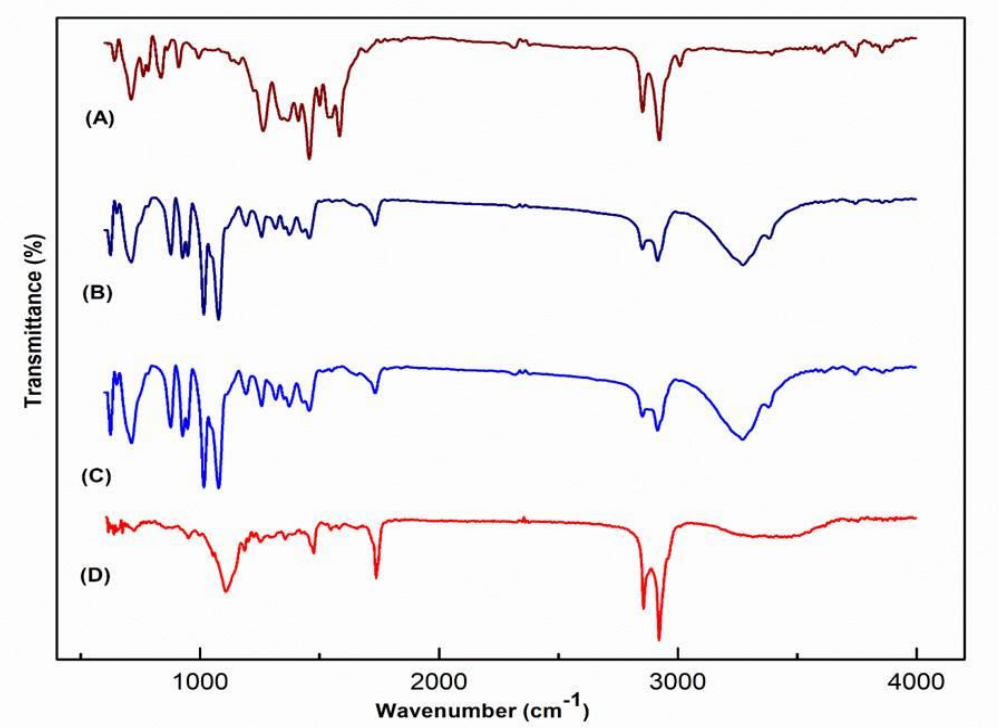

Figure 7.2: FT-IR spectra of $Ana_{C15:3}$ (A), $Ana_{C15:3}$-SLNs (B), and Blank SLNs (SLNs without $Ana_{C15:3}$ (C) and $Ana_{C15:3}$-SLNs-CH-DNase (D)

7.3.1.5 X-ray diffraction study

X-ray diffraction pattern of $Ana_{C15:3}$, excipients, and $Ana_{C15:3}$ encapsulated formulations is displayed in Figure 7.3. $Ana_{C15:3}$ exhibited intense peaks at diffraction angles (2θ) 9.02, 13.4, 17.9, 20.2, and 22.8, suggesting the crystalline nature of the compound. However, the reduced intensity or absence of intense peaks of $Ana_{C15:3}$ in the XRD spectra of $Ana_{C15:3}$-SLNs and $Ana_{C15:3}$-SLNs-CH-DNase was observed. This might be attributed to the transition of $Ana_{C15:3}$ from crystalline to amorphous upon encapsulation into SLNs.

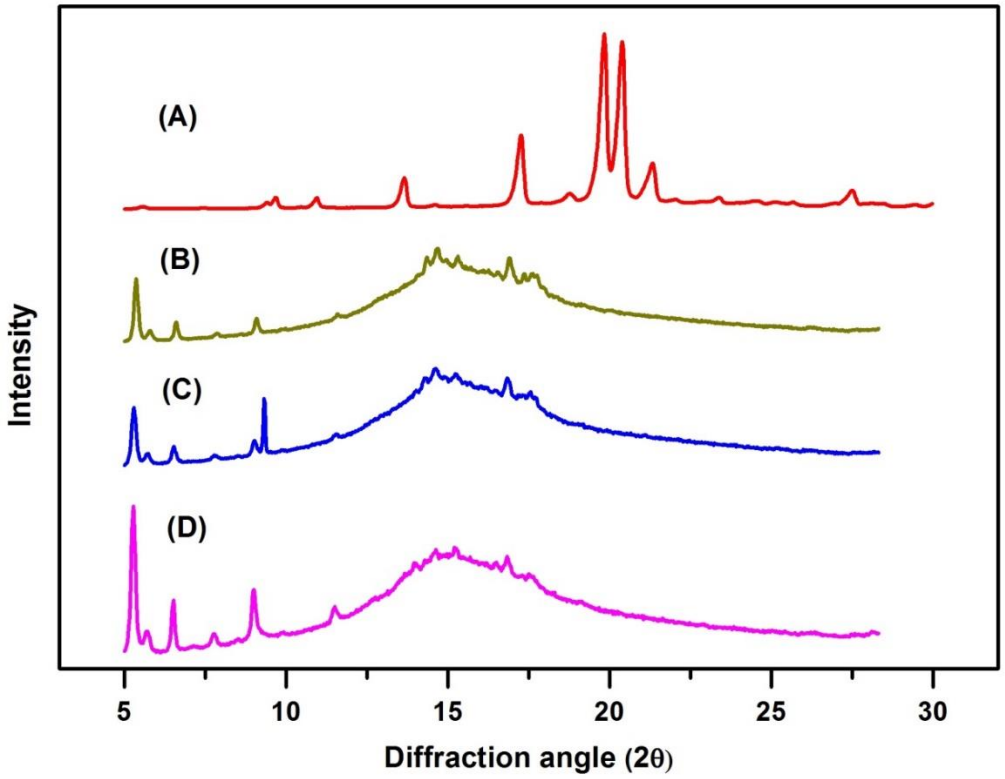

Figure 7.3: XRD plots of $Ana_{C15:3}$ (A), Blank SLNs (SLNs without $Ana_{C15:3}$) (B) and $Ana_{C15:3}$-SLNs (C) and $Ana_{C15:3}$-SLNs-CH-DNase (D)

7.3.1.6 In-vitro drug release study

In-vitro release profiles of $Ana_{C15:3}$ and $Ana_{C15:3}$-SLNs-CH-DNase are depicted in Figure 7.4. The drug release from Ana-suspension was 86.19±3.71% within 6 h and 89.24±3.98% within 24 h while $Ana_{C15:3}$-SLNs-CH-DNase exhibited initial burst release (29.30±1.27 % within one hour) followed by a sustained release for up to 24 h (74.86±2.73 % of total $Ana_{C15:3}$ release, respectively). Further, the drug release kinetics data indicated that $Ana_{C15:3}$-SLNs-CH-DNase followed diffusion controlled drug release mechanism (demonstrated Higuchi model; R^2 0.9724). Higuchi model was found to best fit with an R^2 value of 0.9724, the results were as per the expectation because the drug entrapped in the lipid matrix is hydrophobic therefore the theory erosion of matrix in the buffer solution can be ruled out (Bravo, Duque et al. 2017). We can therefore conclude

that the drug release was possibly due to the diffusion and dissolution of the drug out of the matrix.

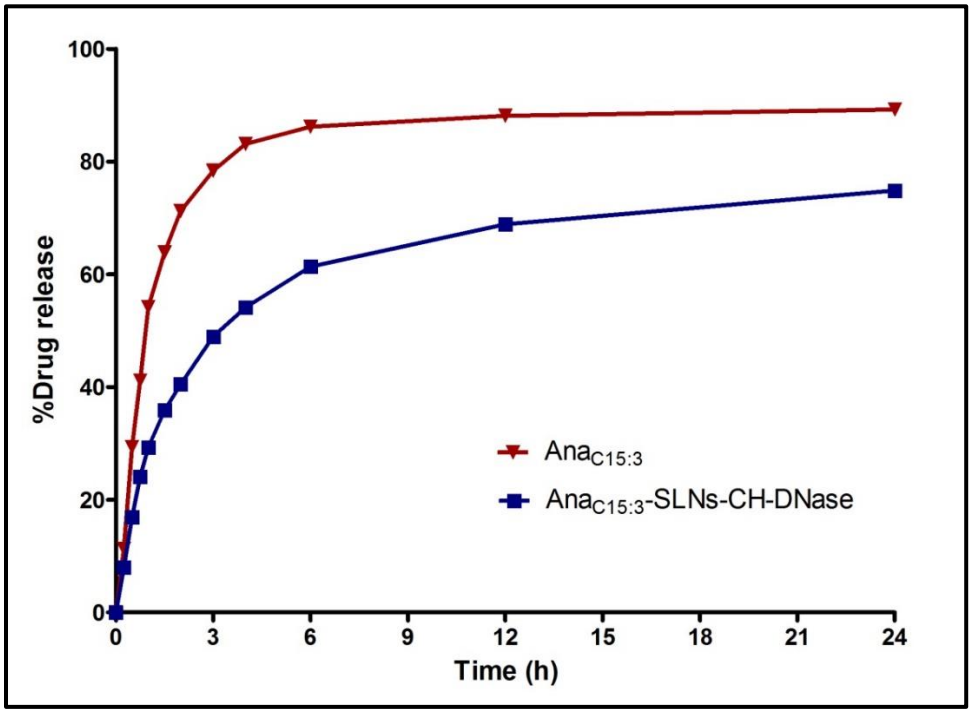

Figure 7.4: Plot indicates the cumulative amount of Ana$_{C15:3}$ release on Y axis with respect to time on X axis from the Ana$_{C15:3}$ and Ana$_{C15:3}$-SLNs-CH-DNase in phosphate buffer (PBS, pH 6.8) as release media containing 0.1% SLS to maintain the sink conditions.

7.3.1.7 Stability studies

From the data demonstrated in

Table **7.3**, the increase in particle size while a decrease in EE% was observed with respect to time. At refrigerated temperature conditions, the SLNs were found to be more stable as the change in particle size as well as encapsulation efficiency were lesser in comparison with storage at room temperature. Results indicate that the final formulation (Ana$_{C15:3}$-SLNs-CH-DNase) was stable, with no aggregation of particles and an insignificant change in EE% during 90 days of the stability study.

Table 7.3: Illustration of variation in particle size and encapsulation efficiency following the storage of SLNs at different temperature conditions.

Day	Refrigerated Condition (2-8 °C)		Room Temperature (25±2°C & 65±5%RH)	
	Particle Size (nm)	Entrapment Efficiency (%)	Particle Size (nm)	Entrapment Efficiency (%)
0	212.8±4.21	73.8±1.23	212.8±4.21	73.8±1.23
30	214.3±3.19	72.7±1.25	217.7±3.45	71.5±1.28
60	217.6±3.48	71.6±1.02	221.8±5.14	70.8±1.36
90	218.6±7.5	71.1±1.19	224.5±6.87	70.2±1.38

7.3.1.8 In-vitro cytotoxicity study

The cytotoxicity study was employed to determine the cell viability of HaCaT cells following the different treatments. The data shown in Figure 7.5 revealed that none of the treatments showed a significant reduction in cell viability even at the highest tested concentration corresponding to the $Ana_{C15:3}$.

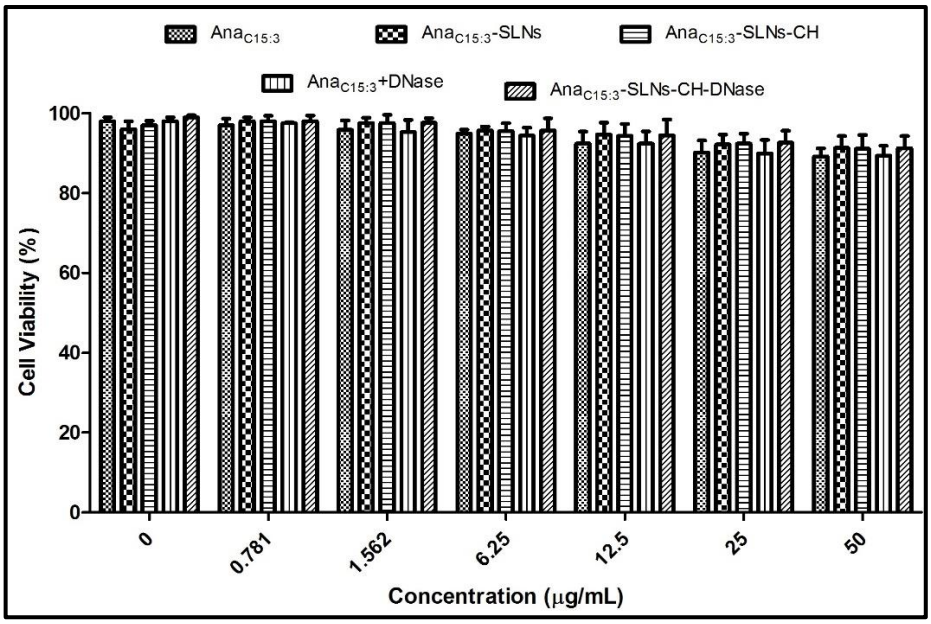

Figure 7.5: Bar diagrams representing the results of the *in vitro* toxicity study (MTT assay). Data are represented as mean±SD (n=3). No significant differences were observed

among the different treatments (One-way ANOVA followed by Newman keul's post hoc test).

7.3.2 Antimicrobial study

The antimicrobial activity of different formulations of $Ana_{C15:3}$ was assessed against *S. aureus* using varying concentrations of $Ana_{C15:3}$. The MIC of $Ana_{C15:3}$ (free) was 0.78 µg/mL, whereas for $Ana_{C15:3}$ formulations (Ana-SLNs, Ana-SLNs-CH, and Ana-SLNs-CH-DNase) it was found to be 1.56 µg/mL. The MIC value of Ana-SLNs is higher than that of free Ana and could be ascribed to the controlled release of Ana from SLNs which may resulted in exposure of *S. aureus* to a lesser concentration of Ana.

7.3.2.1 Effect of SLNs on the formation of biofilm (Evaluation of biofilm inhibition potential)

As depicted in Figure 7.6, biofilm inhibition was observed with all the tested concentrations and both free $Ana_{C15:3}$ and $Ana_{C15:3}$ formulations revealed the considerable magnitude of biofilm inhibition. The biofilm inhibition activity of both free $Ana_{C15:3}$ and $Ana_{C15:3}$ loaded SLNs were observed to be concentration-dependent. Moreover, even at the lowest concentration (0.097 µg/mL), biofilm inhibition was about 55%, while the biofilm growth was completely inhibited at higher concentrations (> 3.125 µg/mL). SLNs ($Ana_{C15:3}$-SLNs, $Ana_{C15:3}$-SLNs-CH, and $Ana_{C15:3}$-SLNs-CH-DNase) revealed slightly decreased biofilm inhibition activity as compared to free Ana at the same range of drug concentration.

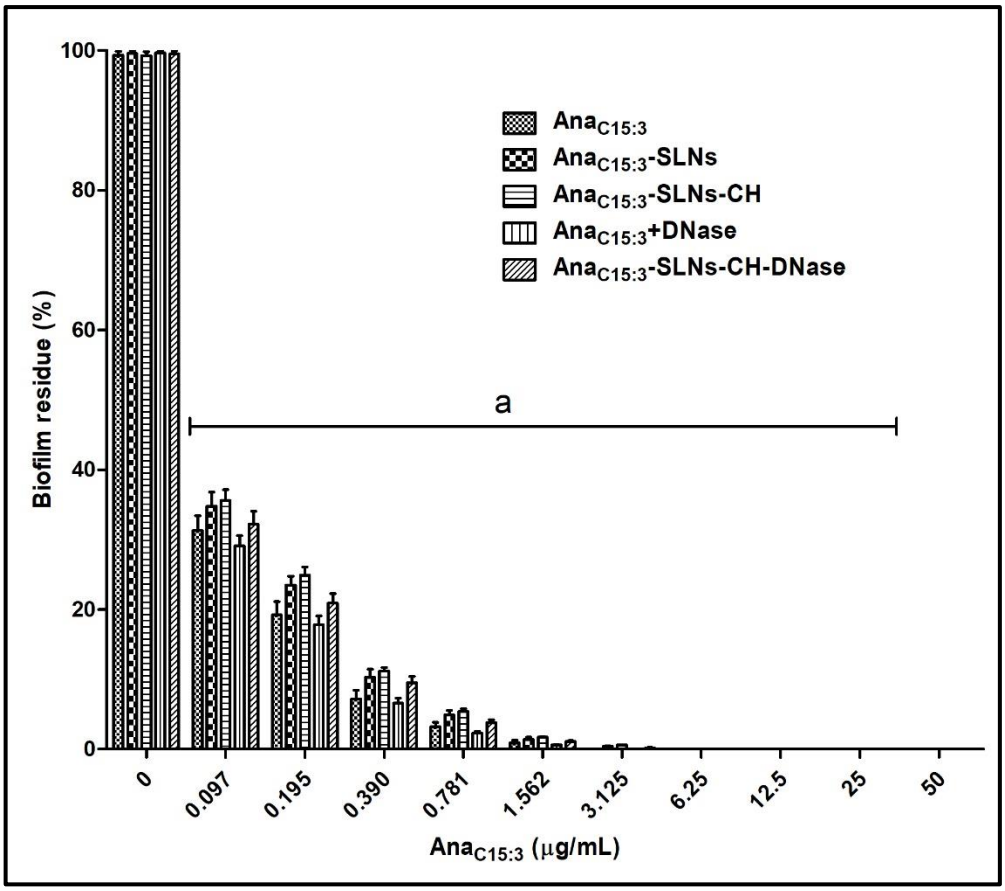

Figure 7.6: Inhibition of *S. aureus* biofilm formation following the different treatments. Graph represents the percentage biofilm residue following the treatment with different concentration of Ana. The results are presented as the mean ± standard deviation of three replicates from three independent experiments. Two-way ANOVA was performed (where [a] represents $p < 0.05$ in comparison with biofilms not receiving any treatment i.e. concentration of $Ana_{C15:3}$= 0 µg/mL). The viable cell count in the control experiments without Ana was $2.41\times10^{9}\pm1.09\times10^{8}$ CFU/mL.

7.3.2.2 Effect of SLNs on mature biofilm (Evaluation of biofilm eradication potential)

Established *S. aureus* biofilm (48 h old) showed a decrease in biofilm residue in dose-dependent pattern upon treatment with SLNs containing DNase ($Ana_{C15:3}$-SLNs-CH-DNase) while activity was lesser with SLNs without DNase ($Ana_{C15:3}$, $Ana_{C15:3}$-SLNs, $Ana_{C15:3}$-SLNs-CH) (Figure **7.7**-A). Free $Ana_{C15:3}$, $Ana_{C15:3}$-SLNs, and $Ana_{C15:3}$-SLNs-CH showed a reduction in biofilm residue as it drops down to 4.80±0.18, 11.85±0.72, and

9.95±0.46% at the highest concentration of $Ana_{C15:3}$ (i.e. 50 µg/mL). $Ana_{C15:3}$-SLNs-CH-DNase showed biofilm detachment up to 36.40±2.38% at the lowest concentration (0.097 µg/mL), while no biofilm residue was observed at $Ana_{C15:3}$ concentrations 6.25 µg/mL and above, suggesting the highest biofilm eradication activity following single-dose treatment. Ana-SLNs-CH revealed penetration into the biofilm, which indicates the ability to bind the biofilm as well as bacterial cells inside the extracellular matrix of the biofilm. As biofilm components are negatively charged, SLNs bearing positive charge could easily attach to the biofilm matrix components like e-DNA (Nafee, Husari et al. 2014). Furthermore, chitosan can make the SLNs penetrate the biofilm matrix and promote $Ana_{C15:3}$ diffusion. Both $Ana_{C15:3}$ and $Ana_{C15:3}$ encapsulated SLNs inhibit biofilm formation, however, the effect of $Ana_{C15:3}$ encapsulated SLNs is somewhat lower as compared to free $Ana_{C15:3}$. This is because encapsulating $Ana_{C15:3}$ in SLNs triggered controlled drug release leading to lesser free drug concentration and decreased antibacterial activity. The DNase used alone or incorporated into the SLNs did not show significant inhibition or increased effect, which might be because DNase acts on the developed biofilms and the drug act on planktonic bacteria directly. In the case of mature biofilm, DNase alone could not exhibit significant antibiofilm activity, which might be because of the dispersed bacterial cells which may again form biofilm until being killed.

7.3.2.3 Antibiofilm activity after repeated doses

As observed earlier, SLNs with DNase ($Ana_{C15:3}$-SLNs-CH-DNase) showed higher biofilm eradication activity in removing *S. aureus* biofilm in comparison with free $Ana_{C15:3}$ and other formulations without DNase (Figure **7.7**-B). In this study, we evaluated the potential of disassembling 48 h old biofilm with repeated treatment of free $Ana_{C15:3}$ and SLNs formulations (one dose per day for two consecutive days) (Figure **7.7**-B). After 48 h of treatment, it was observed that $Ana_{C15:3}$-SLNs-CH-DNase depicts the

highest antibiofilm activity (100% eradication at $Ana_{C15:3}$ concentrations 3.125 µg/mL onwards). Moreover, the free $Ana_{C15:3}$, $Ana_{C15:3}$-SLNs, and $Ana_{C15:3}$-SLNs-CH also showed a reduction in biofilm as it decreased to 19.81±1.28, 16.54±1.21, and 15.18±1.05 % at the Ana concentration 3.125 µg/mL. The inclusion of DNase resulted in the enhanced anti-biofilm activity. SLNs coated with chitosan and DNase hold the promise to increase the penetration and distribution of antibiotics into biofilms while increasing biofilm eradication as an additional effect of DNase and chitosan. $Ana_{C15:3}$-SLNs-CH alone showed a promising extent of biofilm eradication, however, the antibacterial activity of $Ana_{C15:3}$ was greatly improved in the presence of DNase. The addition of DNase in the formulation demonstrated high anti-biofilm capacity, indicating a synergistic effect. This could be attributed to the improved mobility of SLNs, because the enzyme is actively degrading the e-DNA of the biofilm matrix. The similar findings were reported by Messiaen et al. 2013 with 10-fold enhanced diffusional rate of charged polymeric nanoparticles in biofilm, in the presence of DNase (Messiaen, Forier et al. 2013). Moreover, remarkable higher biofilm suppression was obtained when SLNs bearing both chitosan and DNase at the same time were used ($Ana_{C15:3}$-SLNs-CH-DNase). These results demonstrate that drug delivery utilizing e-DNA degrading SLNs may penetrate better into the bacterial colony, and damage biofilm integrity more efficiently. Moreover, the degradation of bacterial e-DNA is known to disassemble the structure of the bacterial ECM, which in turn loosens up and becomes more permeable, leading to improved antibiotic efficacy.

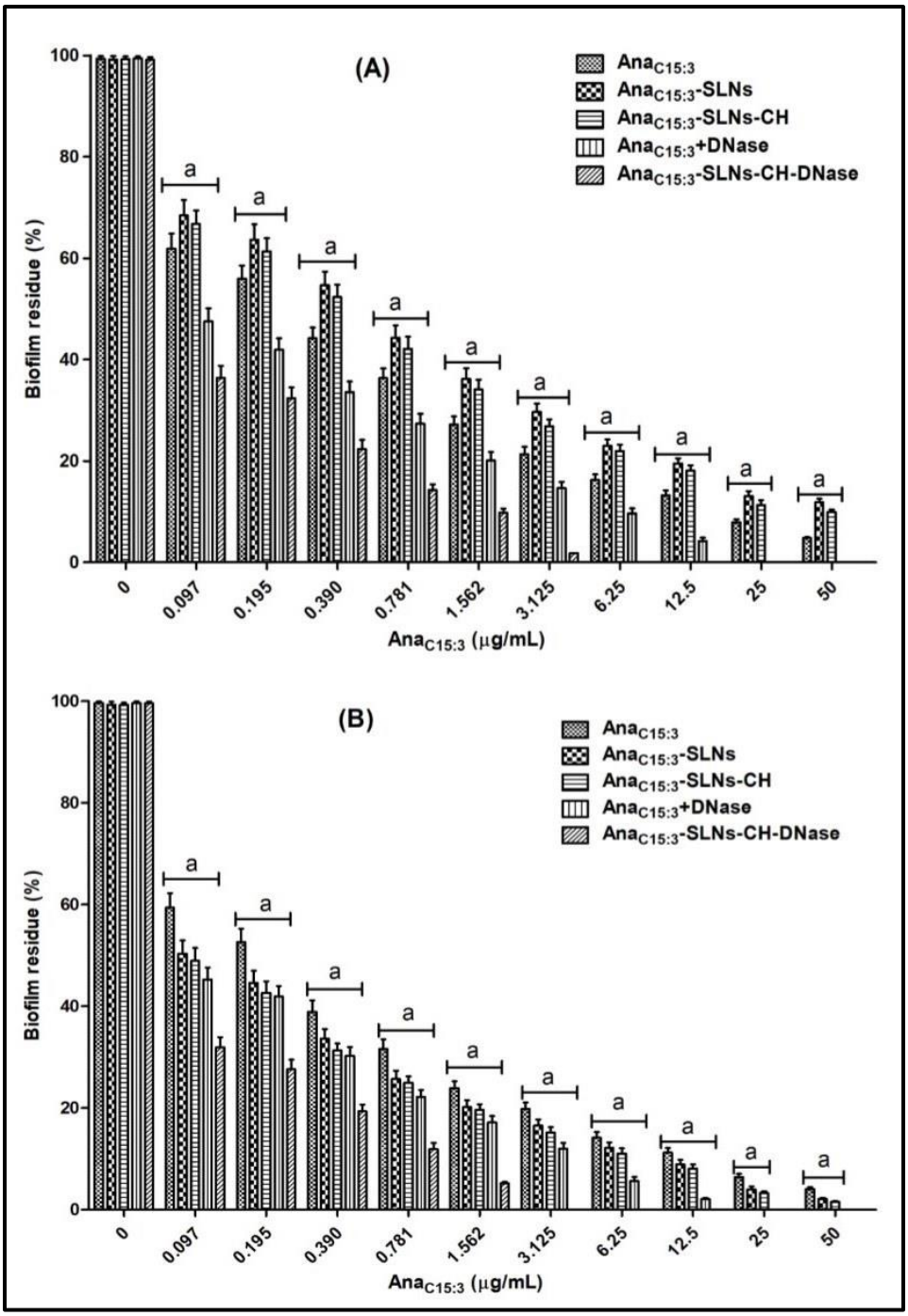

Figure 7.7: Disassembling of mature biofilm following the treatment with a single dose (A) and repeated dose (B). The data represents the percentage of biofilm residue that remained following the treatments. The values are expressed as mean ± standard deviation of three replicates from three independent experiments. Two-way ANOVA was performed (where [a]represents $p < 0.05$ as compared with Ana$_{C15:3}$-SLNs-CH-DNase). The viable cell count in the control experiments without Ana$_{C15:3}$ was $2.91\times10^{9}\pm1.13\times10^{8}$ CFU/mL

7.3.2.4 Microscopic study of biofilm

To confirm the biofilm disassembling potential of free $Ana_{C15:3}$ and developed SLNs on 48 h old *S. aureus* biofilm, a microscopic study was performed by application of the test samples on biofilm grown on the coverslip in culture plate (12 well). The data, presented in Table 7.4, demonstrates the biomass and thickness, which were determined from z stack CLSM images (Figure 7.8; A-F) employing COMSTAT 2 software.

Table 7.4: Data displaying biomass and thickness of biofilm upon treatment with different formulations.

	Biomass ($\mu m^3/\mu m^2$)	**Thickness (µm)**
Control (Without treatment)	27.77± 1.58$^{\#}$	50.30 ± 2.5$^{\#}$
$Ana_{C15:3}$ (Free)	21.86 ± 1.86$^{*\#}$	33.93 ± 2.35$^{*\#}$
$Ana_{C15:3}$ +DNase	16.18±1.11$^{*\#}$	21.81±1.23$^{*\#}$
$Ana_{C15:3}$ -SLNs	17.95±1.29$^{*\#}$	24.82±1.86$^{*\#}$
$Ana_{C15:3}$ -SLNs-CH	16.39±1.26$^{*\#}$	23.27±1.68$^{*\#}$
$Ana_{C15:3}$ -SLN-CH-DNase	10.54±1.53*	18.61±1.21*

All the data represented as mean ± SD (n=3), * represents a significant difference as compared to control while # denotes a significant difference compared with Ana-SLN-CH-DNase. ($p<0.005$, one-way ANOVA followed by Newman-Keuls Multiple Comparison Test).

The control group without any treatment demonstrated the highest biomass and thickness. All the test samples showed an inhibitory effect on biofilm and a reduction in its biomass and thickness upon the treatment. $Ana_{C15:3}$-SLNs-CH-DNase revealed a maximum reduction in biomass and thickness (10.54±1.53 $\mu m^3/\mu m^2$ and 18.61±1.21 µm, respectively) in comparison with control. In line with our hypothesis, $Ana_{C15:3}$+DNase, $Ana_{C15:3}$-SLNs, and $Ana_{C15:3}$-SLNs-CH were more effective than free $Ana_{C15:3}$ (Table 7.4). This interpretation of anti-biofilm efficacy of the $Ana_{C15:3}$-SLNs-CH-DNase is strengthened by the CLSM study, which indicates that DNase-coated SLNs, apart from being more effective at eradicating bacterial cells (exhibited reduction in biomass),

consistently reduced the thickness of the biofilm, indicating the ability of the SLNs to disassemble the extracellular matrix and allowed increased efficacy of $Ana_{C15:3}$ to kill the bacterial cells (Baelo, Levato et al. 2015). The impact of this effect is even more important when considering a longer treatment of an established biofilm infection. With repeated daily administrations of this SLNs formulation, biofilm biomass and thickness reduction were steadily improved.

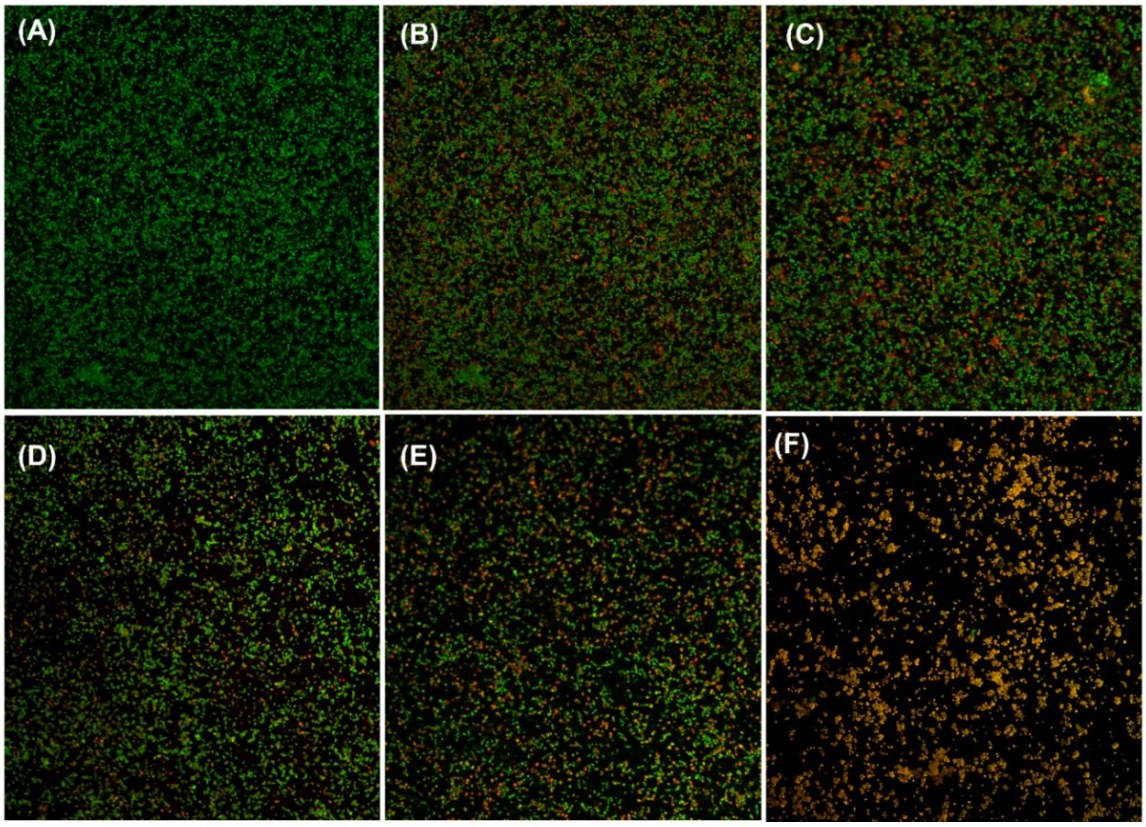

Figure 7.8: CLSM image showing *S. aureus* biofilm formation without any treatment (A) and following the treatment with $Ana_{C15:3}$ (B), $Ana_{C15:3}$-SLNs (C), $Ana_{C15:3}$-SLNs-CH (D), $Ana_{C15:3}$+DNase (E), and $Ana_{C15:3}$-SLNs-CH-DNase treatment. The cells of the biofilm were stained using the Live/Dead Backlight™ bacterial viability kit. CLSM images demonstrate the staining pattern of live cells (SYTO-9, green) and dead cells (propidium iodide, red).